Threshold Fracture of Lightly Cross-Linked Networks

K. A. Mazich,* M. A. Samus, C. A. Smith, and G. Rossi

Polymer Science Department, Ford Motor Company, P.O. Box 2053, Drop 3198, Dearborn, Michigan 48121

Received September 21, 1990; Revised Manuscript Received December 14, 1990

ABSTRACT: Threshold fracture energy, G_0, is reported for several lightly cross-linked PDMS networks. The average length between chemical junctions, ζ_c, characterized with statistical theory, is much greater than the average length between entanglement points, ζ_e, for PDMS in each network. Data indicate that the dependence of G_0 on ζ_c for lightly cross-linked networks is much weaker than the classic form, $\zeta_c^{1/2}$. We discuss two alternative limiting expressions for G_0 based on the role of trapped entanglements on the fracture mechanisms.

Introduction

Fracture resistance in polymeric materials is generally attributed to two major mechanisms that absorb or dissipate energy as cracks advance through the system of polymer chains. A primary contribution stems from the energy required to extend polymer chains, or some subsection of the chains, to the point of rupture.[1,2] The energy requirement for this chain-breaking mechanism contains two terms: (1) extensional energy is needed to deform the chain to a fully extended configuration and (2) each of the main-chain bonds along this fully extended chain will store its rupture energy (or dissociation energy) before the chain breaks. The contribution of the rupture energy is generally the dominant term to the total energy dissipated. In this fracture mechanism, chains that lie in the fracture plane are successively ruptured as the crack advances through the material.

A second, very important contribution to fracture resistance stems from viscous dissipation. Viscoelastic loss associated with chain deformation in regions around the crack tip is a primary mechanism of fracture resistance in polymers.[3-6] The contribution of this process depends on crack velocity and temperature and often follows simple superposition schemes.[6-8] Dissipation is also attributed to a pulling, or "suction", of chains from the surrounding polymer matrix across the fracture plane.[9] This is a direct process of dissipation, generally confined to the fracture plane.

The relative contribution of these mechanisms of fracture resistance depends on the time scale of the fracture process.[10] This time scale is defined by the crack velocity. Minimization of viscoelastic loss and suction energy is expected at high velocity (low temperature) in glasses or at very low rates (high temperature) for systems with an equilibrium structure, i.e., polymer networks. At finite rates, viscoelastic processes and chain suction will augment the fracture resistance of the polymer system.

In this paper, we center on the chain-breaking mechanism of fracture in lightly cross-linked polymer networks. Such networks contain relatively long elastically active chains; the average spacing between chemical junctions in the network, ζ_c, is many times longer than the average spacing between entanglement loci, ζ_e. (ζ_c and ζ_e are defined as the average number of main-chain steps between respective interaction points.) Networks are randomly cross-linked, and every primary chain has a large number of contacts with monomers that belong to neighboring chains. In this case, a mean-field theory can be used to characterize the average size of network structures.[11] Here, we use the statistical theory of Pearson and Graessley[12] to calculate the size of elastically active chemical chains in several lightly cross-linked polymer networks.

The chain-breaking mechanism of fracture in networks involves only the elastically active structures contained in the network. Network imperfections completely relax to the rest state for sufficiently long time scales (i.e., sufficiently slow crack velocity). Fracture under these conditions is commensurate with the threshold fracture energy, G_0. The classic form of the Lake–Thomas[1] theory predicts that $G_0 \sim \zeta_c^{1/2}$ for a perfect network with $\zeta_c \leq \zeta_e$. This theory correctly describes the threshold fracture energy of networks when $\zeta_c \leq \zeta_e$. However, for a lightly cross-linked network with $\zeta_c \gg \zeta_e$, we previously showed that the effective chain length for threshold fracture correlates with ζ_e.[13] This suggests that G_0 depends on trapped entanglements in some fashion and will not increase without bound as $\zeta_c^{1/2}$. Here, we present experimental data on the chemical spacing dependence of G_0. We extend the analysis to several networks with differing cross-link densities but maintain the condition $\zeta_c \gg \zeta_e$. We also give several simple theoretical forms for threshold fracture energy that are derived for model situations. These results are discussed and compared with experimental data.

Experimental Materials and Methods

The materials and methods used in this study are reported in ref 13. A brief account of the experimental program is given here.

Poly(dimethylsiloxane) (PDMS) samples from Dow Corning Corp. were used as received. From gel permeation chromatography, M_w = 592 000 and M_n = 400 000. Pure shear specimens were molded with PDMS according to methods described previously; various amounts of bisperoxide [1,4-bis(2-*tert*-butylperoxyisopropyl)benzene] were used to cross-link the networks.

The measured sol fraction and primary molecular weight distribution were used with results from Pearson and Graessley's[12] statistical calculations to characterize the average lengths of structural features in the networks. The average chemical spacing, ζ_c, the average length of dangling chain ends, ζ_d, and the density of elastically active chemical chains, ν_c, are given in Table I. As expected, increasing the amount of cross-linking agent produces smaller chemical spacing and greater elastically active chain density.

Mechanical characterization of the networks was performed with linear viscoelastic measurements on a Rheometrics mechanical spectrometer Model RMS-800. Dynamic mechanical data were collected with parallel plates, 25 mm in diameter. An Instron servohydraulic Model 1350 was used to measure stress-relaxation data at moderate strains for each network. Samples were strained in pure shear up to λ = 1.5. Data were fit with the Thirion and Chasset[14] equation, and stress at $t = 10^5$ s was used to construct "equilibrium" stress–strain curves. Strain energy density, W_0, was found from the area under these curves.

0024-9297/91/2224-2766$02.50/0

Table I

network	bisperoxide, %	s	$\alpha \times 10^3$	$\nu_c \times 10^{-19}$	ζ_c	$\nu_{end} \times 10^{-19}$	ζ_{end}
SXOP3	0.3	0.114	0.445	0.156	3960	0.186	4220
SXOP5	0.5	0.123	0.428	0.144	4140	0.180	4400
SX1P0	1.0	0.106	0.462	0.169	3800	0.191	4040
SX1P2	1.2	0.048	0.679	0.340	2560	0.234	2720

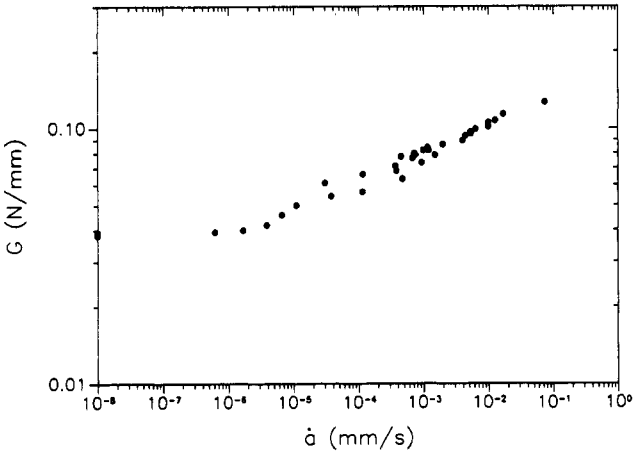

Figure 1. Fracture energy, G, vs crack velocity, $\dot{a}$, for network SXOP3. T = 24 °C.

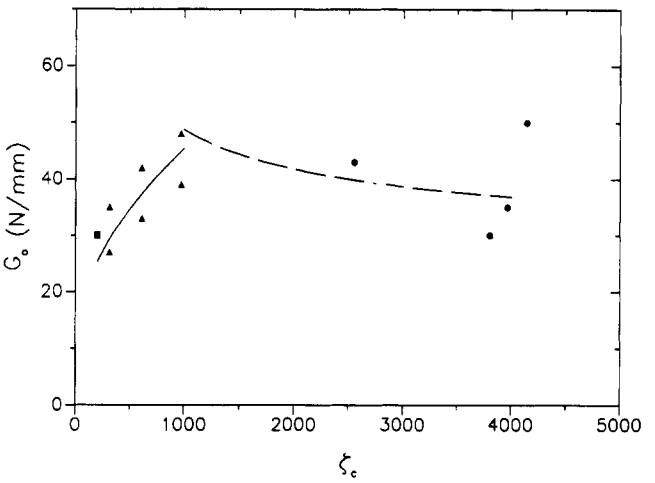

Figure 2. Threshold fracture energy, G_0, vs the elastically active chemical chain spacing, ζ_c. Symbols correspond to data measured by the following work: Mazich, et al. (●), Gent and Tobias[15] (▲), Yanyo and Kelley[16] (■).

Fracture experiments were performed on the pure shear specimens. A notch was formed on one end and a step strain was subsequently applied. Crack length, measured in the undeformed state, was measured as a function of time. Crack length generally increased linearly with time, as required by the Rivlin–Thomas[3] analysis of notched pure shear specimens. The fracture energy, G, was calculated with eq 1,

$$G_0 = W_0 h_0 \tag{1}$$

where h_0 is the undeformed specimen height. Equation 1 represents an energy balance on the notched pure shear specimen for an incremental change of crack surface area. We assume that a volume of material, equal to $A_0 h_0$, transfers to the completely relaxed state (from W_0 to $W = 0$) as the crack advances and creates new surface area, A_0 (referred to the undeformed sample dimensions).

Experimental Results

Network Characterization. Calculation of the average chemical spacing, ζ_c, for each of the PDMS networks was performed with Pearson and Graessley's[12] statistical theory. The distribution of primary-chain molecular weight was assumed to follow the Schulz distribution. Results of the characterization are given in Table I. Networks are identified by the weight percent of bisperoxide used to cross-link the network.

As expected, the average chemical spacing increases with decreasing cross-link density (i.e., decreasing fraction of cross-linked monomer units, α). From viscoelastic characterization of PDMS, ζ_e is approximately 270 main-chain steps. Comparing ζ_e with the values for ζ_c in Table I, we conclude that the chemical spacing for these networks is from 10 to 15 times longer than ζ_e. We also note that the elastically active chain density is roughly equal to the dangling chain end density. The length of elastically active chains and dangling ends is also comparable. However, the effects of the dangling ends on our measurements are minimized at long times for PDMS. For perspective, the longest Rouse time for an entangled subchain is approximately 10^{-7} s at room temperature.

Fracture Energy. The fracture energy, G, of a polymer network generally varies with crack velocity. This dependence is attributed to the rate dependence of the dissipation mechanisms available to the network. In Figure 1, we present sample data of G vs crack velocity, $\dot{a}$, for network SXOP3. This network contains rather long network imperfections (e.g., dangling ends) that dissipate energy over much of the time scale shown in Figure 1. Results for the other networks showed similar qualitative behavior. However, the rate of increase of G with $\dot{a}$ was greater for networks with longer imperfections and greater sol fraction.

As $\dot{a} \to 0$, a plateau value for G is observed in the data. Viscoelastic dissipation is minimized at these velocities, and the time scale of the fracture event now surpasses the time scales of relaxation for the various network imperfections. Several data points are also plotted along the G axis. These points represent experiments in which the notch did not advance for a period of at least 3 days. The value of G on the graph corresponds to the applied strain energy in these experiments. These data points correlate with the plateau region defined by the results at finite velocity and suggest that the plateau truly represents a limiting value for G. We conclude that the plateau in Figure 1 provides a good measurement of the threshold fracture energy, G_0.

From similar plots of G vs $\dot{a}$, we determined G_0 for each of the lightly cross-linked networks. In Figure 2, G_0 is plotted vs the chemical spacing, ζ_c, for each network. The range of ζ_c shown in the figure extends well beyond $\zeta_e \sim$ 270 main-chain steps. Data reported by Gent and Tobias[15] and Yanyo and Kelley[16] are also plotted for comparison. Their data were collected for end-linked networks, where the chemical spacing is well-known. Gent and Tobias[15] used their data to verify the $\zeta_c^{1/2}$ dependence for G_0 predicted by the classic Lake–Thomas theory.[1] As shown in Figure 2, this result is applicable for $\zeta_c \sim \zeta_e$. (A solid line that represents the $\zeta_c^{1/2}$ dependence is shown in Figure 2.) Our data at high ζ_c clearly show that this dependence no longer holds for lightly cross-linked networks when $\zeta_c \gg \zeta_e$. This result supports the conclusion that trapped entanglements play an important role in threshold fracture of lightly cross-linked networks. Some

form other than $\zeta_c^{1/2}$ is required to model data in this range of chemical spacing.

We should note that the data presented in Figure 2 correspond to network systems with a single (average) value for ζ_c and a characteristic value for ζ_e. Gent and Tobias[17] prepared systems where two networks with different values of ζ_c were interlinked with each other at a common interface. The bonding strength of the interface was provided by loops of one network entangled with the other. The strength of these samples under threshold conditions depends on the local concentration of each chain type at the fracture plane and on the values of ζ_c for the respective networks. Such interlinked networks provide interesting combinations of the parameters (effective chain crossings of the fracture plane, effective chain length for fracture) that are used to estimate the threshold fracture energy in the discussion below.

Discussion

In the threshold fracture energy of a polymer network, the chain-breaking mechanism is the only means of fracture resistance. Data suggest that the effective chain length involved in this mechanism depends on the relative lengths of the chemical chain and trapped entangled chain. Here, we derive some expressions for G_0 based on several simple assumptions of the network structure. These assumptions yield analytical forms for G_0 that can be compared with experimental data.

Theories for chain-breaking fracture energy[1] generally count the number of effective chains per unit area, ξ^*, and multiply by the rupture energy per effective chain, U^*

$$G_0 = \xi^* U^* \tag{2}$$

Extensional energy can be neglected since this contribution is small.[10] The rupture energy, U^*, depends linearly on the effective chain length, ξ^*, since each bond in the effective chain is strained to rupture before the chain breaks. The effective chain crossings per unit area are proportional to $\nu_{eff} l$, where ν_{eff} is the effective chain density and l is a characteristic length of the system in the undeformed state. For Gaussian chains, $l \sim \zeta_c^{1/2}$.

Typically, ν_{eff} is written as $\nu_{eff} \sim 1/\zeta^*$.[1,18] This is strictly correct only if every chain in the network has length ζ^* and is elastically active. When $\zeta^* = \zeta_c \leq \zeta_e$, these assumptions give the classic form of the Lake–Thomas theory,[1] $G_0 \sim \zeta_c^{1/2}$. This describes a "perfect" network that approximates the systems studied by Gent and Tobias.[15] As discussed above, this function correctly models G_0 when $\zeta_c \leq \zeta_e$ but fails as ζ_c surpasses other characteristic dimensions of the system such as ζ_e. Note that the assumption that every chain is elastically active is not essential for the Lake–Thomas form.[1] Corrections for imperfections are generally small for these "tightly" cross-linked networks, and the $\zeta_c^{1/2}$ dependence also models data for imperfect networks, e.g., randomly cross-linked networks.

Lake and Thomas[1] also considered the contribution of entanglements to the total effective chain density in their original paper. Now, ν_{eff} is written as the sum of the chemical chain density, ν_c, and the entanglement chain density, ν_e. This theory, as developed and tested by Ahagon and Gent,[18] gives the following form:

$$G_0 \sim \left[\frac{1}{\zeta_c} + \frac{1}{\zeta_e}\right]^{-1/2}(1 - \gamma\zeta_c) \tag{3}$$

Several assumptions regarding the network structure are implicit in this derivation: (1) Trapped entangled chains are subsets of elastically active chemical chains, so writing $\nu_{eff} = \nu_c + \nu_e$ counts too many active chains per unit volume. (2) ν_{eff} contains the Flory correction for chain ends based on the chemical spacing; sol fraction is neglected. (3) The length scales l and ζ^* are written assuming all chemical and entangled chains are active.

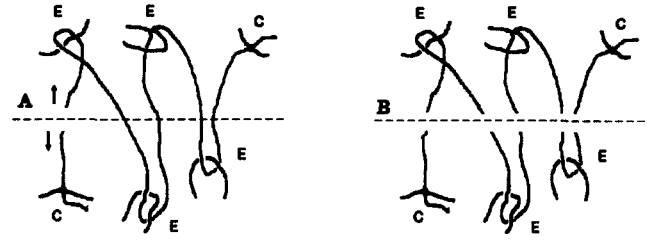

Figure 3. Proposed chain scission through entangled networks. E = trapped entanglement loci and C = chemical cross-links. (A) The first entangled subchain is ruptured, and the remaining chain ends retract across the fracture plane. (B) Each entangled subchain is ruptured in the fracture plane.

G_0 calculated with eq 3 was compared with the experimental data. Good agreement is found around $\zeta_c = \zeta_e$; in fact, eq 3 reduces to $\zeta_c^{1/2}$ when $\zeta_c < \zeta_e$. However, the predicted dependence of G_0 on ζ_c is too strong at high ζ_c. Moreover, we expect $G_0 \to 0$ as $\zeta_c \to \infty$ since this condition stipulates a polymer melt, whereas eq 3 gives a nonvanishing G_0 as $\zeta_c \to \infty$.

New expressions for G_0 can be derived explicitly for networks with $\zeta_c \gg \zeta_e$ by considering trapped entangled chains as the effective chains in threshold fracture. This sets ζ^* equal to ζ_e. We calculate the effective number of chains that cross unit area by assuming that all chemical chains are elastically active and have length ζ_c. This assumption also corresponds to a perfect network, but now the chemical chains are much longer than ζ_e. Two potential situations for chain breaking are related to this model network, as shown in Figure 3. In the first situation (Figure 3A), we claim that several trapped entangled subchains that belong to a given chemical chain will cross the fracture plane. Once the first entangled subchain is severed, the remaining entangled chains along that given elastically active chemical chain are rendered inactive. The dangling ends that result in this case retract back across the fracture plane (depicted by the arrows in Figure 3A) and do not contribute to chain-breaking fracture. This implies that the time scale of the fracture process is really long enough to allow the retraction. Under these assumptions, we simply count chemical chains for ν_{eff} and l, but $\zeta^* = \zeta_e$. Since all chains are equivalent, $\nu_{eff} \sim 1/\zeta_c$ and

$$G_0 \sim \zeta_e/\zeta_c^{1/2} \tag{4}$$

The limiting forms of this expression reduce to correct relationships for G_0, i.e., $G_0 \to 0$ as $\zeta_c \to \infty$ for a melt; when $\zeta_c = \zeta_e$, $G_0 \sim \zeta_c^{1/2}$, which is equivalent to the Lake–Thomas form at ζ_e. The broken curve in Figure 2 represents the result for this model. Equation 4 is fit to the data at $\zeta_c = 1000$ and $\zeta_c = 4000$. The scatter in the data and the small number of data points do not allow careful evaluation. But given the assumptions used in the model (which do not strictly correspond to the experimental networks), agreement is rather good.

A final assumption yields an interesting form for G_0. We use the same picture given above but now assume that the entangled subchains that remain after the first is severed do not retract across the fracture plane. Rather, they are also ruptured as the crack advances through the network (Figure 3B). This mechanism does not strictly comply with fracture at infinitely slow rates (threshold

fracture). However, when the first entangled subchain breaks, the tip of the crack is immediately defined by the next chain in the fracture plane. This next chain might correspond to a second, third, etc., entangled subchain along the same chemical chain. In this case, all entangled subchains that cross the fracture plane must be included in the counting process. Now, we multiply the single-chain case (eq 4) by the number of fracture plane crossings of the chemical chain. The chemical chain contains ζ_c/ζ_e entangled steps, and each is assumed to be Gaussian. Thus, the projection of the random chain on the fracture plane gives $(\zeta_c/\zeta_e)^{1/2}$ intersections, and

$$G_0 \sim \left(\frac{\zeta_c}{\zeta_e}\right)^{1/2} \frac{\zeta_e}{\zeta_c^{1/2}} = \zeta_e^{1/2} \tag{5}$$

This is essentially the result for an entangled polymer glass.[19] G_0 is independent of ζ_c, and all entangled chains are considered active. This form for G_0 is also a reasonable approximation to the existing experimental data shown in Figure 2, as it would correspond to a horizontal line in this plot.

Summary

Experimental data for lightly cross-linked networks containing relatively long elastically active chemical chains clearly indicate that the $\zeta_c^{1/2}$ dependence for G_0 fails for such networks. The ζ_c dependence appears to become much weaker for $\zeta_c \gg \zeta_e$. Considerations of trapped entangled chains are necessary to explain the observations.

Several theoretical expressions are discussed. Each of them accounts for the energy needed to rupture a set of effective chains that cross the fracture plane. Simple assumptions were used to count the number of chains that cross the fracture plane and obtain limiting forms for G_0. In particular, we give two new expressions for a lightly cross-linked perfect network. In one case, entangled subchains are explicitly assumed to account for effective chains, and only one entanglement needs to be ruptured for each elastically active chain. This assumption gives $G_0 \sim \zeta_e/\zeta_c^{1/2}$. In a second case, the crack tip immediately proceeds to the next elastically active subchain. Therefore, additional entangled chains along each elastically active chemical chain contribute to fracture resistance. Then, $G_0 \sim \zeta_e^{1/2}$; this is essentially the result for entangled polymer glass. The scatter in the limited data cannot distinguish these models.

Acknowledgment. We are grateful to Prof. P. Pincus and Dr. H. van Oene for stimulating and helpful discussions on fracture in polymers.

References and Notes

(1) Lake, G. J.; Thomas, A. G. *Proc. R. Soc. London, A* **1967**, *300*, 108.
(2) Mueller, H. K.; Knauss, W. G. *Trans. Soc. Rheol.* **1971**, *15*, 217.
(3) Rivlin, R. S.; Thomas, A. G. *J. Polym. Sci.* **1953**, *10*, 291.
(4) de Gennes, P.-G. *C. R. Seances Acad. Sci. Ser.* **1988**, *307*, 1949.
(5) Andrews, E. H. *J. Mater. Sci.* **1974**, *9*, 887.
(6) Smith, T. L. *J. Polym. Sci.* **1958**, *32*, 99.
(7) Plazek, D. J.; Choy, I.; Kelley, F. N.; von Meerwall, E.; Su, L. *Rubber Chem. Technol.* **1983**, *56*, 866.
(8) Kadir, A.; Thomas, A. G. *Rubber Chem. Technol.* **1981**, *54*, 15.
(9) de Gennes, P.-G. *J. Phys. Fr.* **1989**, *50*, 2551.
(10) Evans, K. E. *J. Polym. Sci., Polym. Phys. Ed.* **1987**, *25*, 353.
(11) de Gennes, P.-G. *Scaling Concepts in Polymer Physics*; Cornell University Press: Ithaca, NY, 1979.
(12) Pearson, D. S.; Graessley, W. W. *Macromolecules* **1978**, *11*, 528.
(13) Mazich, K. A.; Samus, M. A. *Macromolecules* **1990**, *23*, 2223.
(14) Chasset, R.; Thirion, P. *Proceedings of Conference on Physics of Non-Crystalline Solids*; Prins, J. A., Ed.; North-Holland Publishing: Amsterdam, The Netherlands, 1965; p 345.
(15) Gent, A. N.; Tobias, R. H. *Am. Chem. Soc. Symp. Ser.* **1982**, *193*, 367.
(16) Yanyo, L. C.; Kelley, F. N. *Rubber Chem. Technol.* **1987**, *60*, 78.
(17) Gent, A. N.; Tobias, R. H. *J. Polym. Sci., Polym. Phys. Ed.* **1984**, *22*, 1483.
(18) Ahagon, A.; Gent, A. N. *J. Polym. Sci., Polym. Phys. Ed.* **1975**, *13*, 1903.
(19) Mikos, A. G.; Peppas, N. A. *J. Chem. Phys.* **1988**, *88*, 1337.

Registry No. 1,4-Bis(2-*tert*-butylperoxyisopropyl)benzene, 2781-00-2.